Partial oxidation of methane to syngas using NiO-supported catalysts

Russell S. Drago [a], Krzysztof Jurczyk [a], Nicholas Kob [b,*], Alak Bhattacharyya [c] and Joseph Masin [c]

[a] *Department of Chemistry, University of Florida, Gainesville, FL 32611, USA*
[b] *DuPont, Sabine River Laboratory, Orange, TX 77630, USA*
[c] *Amoco Chemical Co., PO Box 3011, Naperville, IL 60566, USA*

Received 7 September 1997; accepted 30 January 1998

Claims for the partial oxidation of methane to CO and H_2 have been clouded by the possibility of the indirect reaction sequence occurring at hot spots in the catalyst bed. In this report, we claim that the direct reaction occurs on NiO/silica at 500 °C with methane conversions as high as 80% and selectivities for H_2 of 80% and CO of 70%. Arguments are presented to show that the amount of diluent gas employed prevents formation of local hot spots with temperatures high enough for the indirect reaction to occur. Consequently, this study constitutes one of the most convincing reports for the conversion of CH_4 to syngas by the partial oxidation of methane. The catalyst deactivates in 10 h. Surface studies show coke formation and aggregation of NiO contribute to the loss of activity.

Keywords: methane, nickel oxide, synthesis gas

1. Introduction

Currently, the steam reforming of natural gas (equation (1)) is the commercial basis for the production of synthesis gas (CO and H_2) [1]:

$$CH_4 + H_2O \rightarrow CO + 3H_2 \quad \Delta H = 49.2 \text{ kcal/mole} \quad (1)$$

The positive free energy of this reaction becomes negative [1] above 618 °C. Steam reforming requires extensive energy input motivating research efforts to develop catalysts for the selective partial oxidation of methane [2–14] to CO and H_2:

$$CH_4 + (1/2)O_2 \rightarrow CO + 2H_2 \quad \Delta H = -8.5 \text{ kcal/mole} \quad (2)$$

As an added benefit, the 2 : 1 ratio of H_2 to CO from partial oxidation is desired for methanol synthesis. Unfortunately, the oxidation of methane to synthesis gas is accompanied by the very exothermic, deep oxidation of methane:

$$CH_4 + 2O_2 \rightarrow CO_2 + 2H_2O \quad \Delta H = -191.8 \text{ kcal/mole} \quad (3)$$

The mechanism of CO and H_2 formation by direct oxidation over a catalyst is reported to proceed through a series of hydrogen dissociation steps [13,14]. CO selectivities are high when the sequence $C_s + O_s \rightarrow CO_s \rightarrow CO_g$ is favored over $CO_s + O_s \rightarrow CO_{2g}$. Hydrogen selectivities are favored by low activation energy barriers for dimerization ($H_s + H_s \rightarrow H_2$), relative to the barriers for water formation.

CO_2 and H_2O, the methane deep-oxidation products, can yield synthesis gas by combining steam reforming (equation (1)) and dry reforming [15–17], i.e., the reaction of methane with CO_2:

$$CH_4 + CO_2 \rightarrow 2CO + 2H_2 \quad \Delta H = 59.0 \text{ kcal/mole} \quad (4)$$

This pathway to syngas is referred to as indirect and requires high temperatures because the free energy of the dry reforming reaction also only becomes negative above 640 °C.

When the oxidation of CH_4 to syngas is carried out at high temperatures, it is difficult to distinguish the direct from the indirect path involving CO_2 and H_2O. At high temperatures, the indirect reaction path is followed by Ni/alumina catalysts yielding methane conversions and CO selectivities close to the equilibrium-controlled amounts [7]. The indirect pathway via steam and dry reforming is the accepted mechanism for catalytic reactions of O_2 [7,10,15] with methane to form syngas above 650 °C.

Below 500 °C, CO and H_2 selectivities much higher than the equilibrium amounts predicted for the indirect process are reported [11] as indicating that the direct, partial oxidation reaction occurs using Ni/Al_2O_3catalysts. The reported reactions are carried out using extremely high space velocities, no diluent gas and an excess of methane to O_2 to prevent total combustion. A later report [12] attributes this claim for direct oxidation to the indirect reaction occurring at local hot spots (1200–1300 °C) generated by high methane conversions at high input.

NiO on alumina is an effective catalyst for the oxidation of methane to synthesis gas [1,8,17]. However, the catalyst deactivates with time on stream by nickel crystallite growth, formation of a spinel, $NiAl_2O_4$ [14] and by carbon deposits [18]. Carbon deposits form from equation (5) and the Boudouard reaction (equation (6)), which is favorable

---

[*] To whom correspondence should be addressed.

© J.C. Baltzer AG, Science Publishers

at the low reaction temperatures (∼200–600 °C) used for the direct oxidation of methane [18]:

$$CH_4 \rightarrow C + 2H_2 \quad \Delta H = 17.93 \text{ kcal/mole} \qquad (5)$$

$$2CO \rightarrow C + CO_2 \quad \Delta H = -41.1 \text{ kcal/mole} \qquad (6)$$

The distribution of H_2 and CO in the products is influenced by the water–gas shift reaction:

$$CO + H_2O \rightarrow CO_2 + H_2 \quad \Delta H = -9.8 \text{ kcal/mole} \qquad (7)$$

This research reports the direct oxidation of methane at low temperatures using a silica-supported nickel oxide catalyst. Experiments are described to establish the direct oxidation path. The effects of nickel oxide loading, support variation, reaction temperature, and deactivation are described.

2. Experimental

2.1. Reagents

Methane, argon and oxygen (both 99.9% purity) were obtained from Matheson Gas Products. Silica gel (100–200 mesh, 350 m^2/g), alumina (80–200 mesh) and titania supports were obtained from Fisher.

2.2. Catalyst preparation and catalytic runs

The various supports were impregnated with the required amount of an aqueous solution of nickel nitrate, dried in a vacuum oven at 100 °C overnight and then calcined at 500 °C in a flowing stream of argon overnight. The feed is started at 500 °C and the temperature was then changed.

All reactions were carried out in a 4 mm id quartz inverted flow mini-reactor using 0.05 g of catalyst supported on a quartz frit. Unless otherwise indicated, flow rates of 30 ml/min methane and 15 ml/min oxygen were fed to the reactor using a calibrated flow meter. The gases were premixed but not heated. The temperature was measured with a thermocouple located just below and in contact with the frit supporting the catalyst bed. These reactions were diluted with 75 ml/min feed of Ar giving a GHSV of 120,000 h^{-1} to minimize formation of hot spots on the catalyst. The steam reforming reaction was carried out in the same flow catalytic reactor except water fed with a calibrated syringe pump and methane were fed in with a 1 : 1 molar ratio. Selectivities to H_2 and CO are given in mole percent, and the other products are CO_2, H_2O and carbon. No alkenes were formed. Catalyst conversions are reproducible to within 5% and product selectivities to 2%.

2.3. Surface analysis

BET analysis was performed using a micromeritics ASAP 2000. X-ray photoelectron spectroscopy (XPS) was done using a Kartos XSAM 800, and samples were mounted on the adhesive side of aluminum tape. The samples were scanned at 90 degrees using Al Kα radiation. The effect of charging was corrected using the Si 2p peak of SiO_2.

3. Results and discussion

In order to avoid catalyst deactivation by spinel ($NiAlO_4$) formation, NiO/silica catalysts were studied in detail for the oxidation of methane to synthesis gas in this study. XPS analysis of this catalyst after activation but before reaction reveals that Ni(0) is not present as a surface species. The metallic Ni peak at a binding energy of 852 eV is absent. The only nickel present on the surface is NiO with its characteristic Ni $2p_{3/2}$ binding energy of 857.1 eV and its satellite peak 6.2 eV away [19]. BET analysis shows no significant drop in surface area upon preparation of the catalyst. Silica gel has a surface area of 350 m^2/g, and a 10% NiO/SiO_2 catalyst has a surface area of 306 m^2/g.

3.1. Catalytic activity

At 500 °C, using 0.05 g catalyst and a 30 : 15 : 75 ml/min $CH_4 : O_2 : Ar$ flow (GHSV of 120,000 h^{-1}), 65–70% conversion of CH_4 with ∼80% selectivity to H_2 and 65% to CO result.

These conversions and selectivity as well as lifetimes show no significant change for NiO loadings of 5 and 18 wt% on silica. A catalyst prepared with 10% NiO and 1% La_2O_3, to catalyze the combustion of coke, led to the deep oxidation of methane to CO_2 and H_2O at the above conditions. It is significant that at these conditions, the indirect reaction is not observed.

3.2. Effect of the support on catalysis

Supports other than silica were investigated, and the results are shown in figures 1 and 2. All catalysts had 18 wt% NiO, the reaction temperature was 500 °C and GHSV was 120,000 h^{-1}. Titania is an ineffective support while silica and alumina are active for the oxidation of methane to synthesis gas. NiO undergoes reduction with H_2 [19(b),20] on

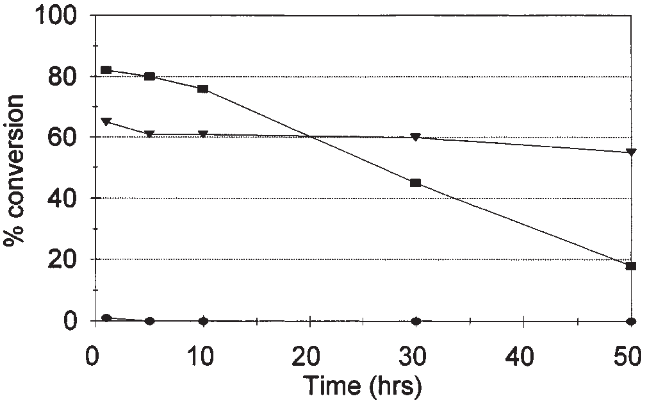

Figure 1. Oxidation of methane with NiO catalysts on various supports. (■) Silica, (▼) alumina, (●) titania.

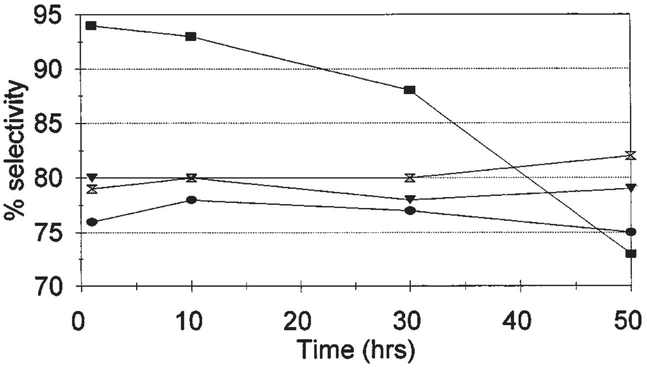

Figure 2. Selectivities for the oxidation in figure 1. (■) H_2 selectivity for NiO on silica; (●) CO selectivity for NiO on silica; (▼) H_2 selectivity for NiO on alumina; (⧖) CO selectivity for NiO on alumina.

different supports with varying degrees of difficulty. It has been shown by XPS that, while NiO exists on silica and alumina supports, Ni^{2+} and Ni^{3+} are detected when NiO is supported on titania [21]. Differences are attributed to support–NiO interactions, and this difference may explain the inability of the titania support to catalyze the reaction.

Silica was selected as the support for further study to overcome spinel formation and achieve greater lifetimes. At the temperatures employed in the support comparison, the alumina-supported NiO is found to be more active than silica after 50 h. Both supports are inactive after 80 h. XPS analysis of the used silica-supported NiO catalyst shows the appearance of a new C 1s peak at 283.1 eV, which is characteristic of graphitic coke [7]. Carbon analyses of the used catalysts also indicate that less than 0.01% of the methane reacted is converted to coke. The XPS intensity ratio of Ni $2p_{3/2}$ to Si 2p (Ni/Si) decreases after 70 h of reaction, indicating aggregation of NiO on the silica. These results are consistent with other XPS results that showed that NiO remains dispersed on alumina better than on silica, with extensive aggregation being common on silica [22]. Carbon analysis after 70 h of reaction revealed that the silica-supported catalyst had 12% carbon, while the alumina catalyst had only 9%. An increased rate of coking [18] and crystallite growth leads to the more rapid loss of activity for the silica- than for the alumina-supported material. This loss in activity negates any benifits that occur with silica by preventing spinel formation.

3.3. Effect of temperature on partial CH_4 oxidations

The effect of reaction temperature on methane conversion and product selectivity was investigated using the 5% NiO on silica catalyst. The results are shown in table 1 and compared to the thermodynamic equilibrium conversions of methane for the direct oxidation process [23].

Table 1
Effect of reaction temperature on catalyst conversions and selectivities.[a]

Temp. (°C)	Conv. CH_4 (%)	Sel. H_2 (%)	Sel. CO (%)	Equilibrium [23] conv. (%)
700	76	85	78	94
500	66	85	69	72
250[b]	38	55	20	54

[a] Reaction conditions: 0.05 g 5% NiO catalyst, 120,000 h^{-1} GHSV. The other product decreasing H_2 selectivity is water and CO_2 decreases CO selectivity.

[b] Temperature lowered from 500 °C.

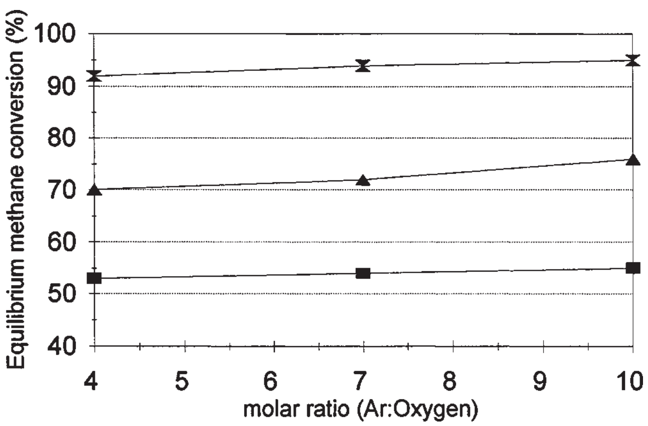

Figure 3. Equilibrium conversions of CH_4 to syngas for the direct oxidation as a function of temperature and argon diluent. (■) 250 °C, (▲) 500 °C, (⧖) 700 °C.

The methane conversion and the CO selectivity obtained at all temperatures are lower than the values predicted by the thermodynamic equilibrium for the partial oxidation of methane to syngas at the given reaction temperature. The equilibrium conversion of methane calculated as a function of temperature and various molar ratios of $Ar:O_2$ with the $CH_4:O_2$ ratio kept constant at $2:1$ is shown in figure 3. The conversion of methane for the direct oxidation at a given temperature is predicted not to decrease as the amount of diluent gas (Ar) increases. This result is confirmed by experiment. Doubling the total gram hourly space velocity (240,000 h^{-1}) by adding more Ar and keeping all other conditions the same as that for the 18% NiO on silica catalyst described above, the conversion of methane was 74%, comparable to that reported in table 1 for 120,000 h^{-1}. The selectivity to H_2 is also similar at 90% while 78% selectivity to CO represents a slight increase.

The steam reforming of methane was studied over the 5% NiO silica catalyst as a control for the indirect pathway. At 700 °C, the 66% conversion of methane observed is similar to that in table 1. However, the 24% conversion at 500 °C and no conversion at 250 °C are significantly lower than that in table 1.

3.4. Direct versus indirect reactions

It is difficult to establish the direct oxidation pathway because high conversions of CH_4 to syngas, CO_2, and H_2O generate substantial heat causing local hot spots that are much higher than the catalyst bed temperature. These hot spots drive the reactions of CO_2 and H_2O with CH_4 and lead to CO and H_2 by the indirect pathway. This is not the case in our experiments because the excess argon diluent gas flow introduced at room temperature removes heat. This conclusion is supported by the following arguments. First, when the external heater temperature is lowered from 700 to 500 °C or from 500 to 250 °C, conversion quickly drops. With the high argon and reactant gas flow introduced at room temperature, the exothermicity of the methane oxidation is not sufficient to maintain bed temperatures. The net of equations (3) and (1) or (3) and (2) is exothermic and, once light-off is achieved, reaction is expected to continue and maintain hot spots if they existed. Second, conversions for the direct oxidation exceeds those for steam reforming at all temperatures. The direct oxidation at 250 °C (table 1) would require catalyst hot spots well above 500 °C to account for the conversion observed in table 1 if the indirect process were involved. It would be difficult to attain and sustain these temperatures in a 75 ml/min room temperature argon flow with 38% conversion. The increase in conversion from 250 to 500 and then to 700 °C parallels the increase expected for the direct oxidation from thermodynamic considerations (figure 3). The slight increase in conversion and CO selectivity upon doubling the flow rate is reasonable for the shorter contact time of the direct oxidation, but is not expected for the indirect process.

The result with 1% La_2O_3 gave 70% conversion of CH_4 to CO_2 and H_2O at 500 °C. This is the most exothermic reaction of the 500 °C runs, and if hot spots formed, they would be most extensive in this experiment and the indirect reaction would have its best chance to occur to produce CO and H_2. As expected, if hot spots do not exist with this argon flow, no products from the indirect reaction are observed.

At the conversions obtained at 700 °C, all the O_2 in the reactants is accounted for by the products formed. In all reported experiments, at 500 °C methane conversions are at levels that ensure that 25% or more of the original O_2 in the reactants is present in the product stream. This would mitigate against the existence of the Ni(0) needed for the indirect mechanism. A recent study [24] of the *in situ* nickel phase as a function of oxygen conversion supports the absence of accessible Ni(0) at the conditions of the 500 °C and lower experiments. Working at 4 : 1 methane to oxygen ratios [24], compared to our 2 : 1, only bulk oxide is detected at oxygen conversion levels of 0 to 25%. At 60%, oxygen conversion nickel(0) crystallites exist but the surface is covered by nickel oxide. This is the expected nickel composition at 500 °C. Redox cycling of NiO is expected for the direct oxidation of methane, and the surface oxide layer would be involved. Reforming occurs over metallic nickel sites.

Finally, in all experiments at these argon flows, including many not reported, the conversions never exceeded those expected from equilibrium considerations for the direct process (figure 3). Local hot spots are indicated when conversions in excess of equilibrium result. Taken together, these results present a compelling argument that hot spots, greatly exceeding reaction temperatures, are not formed at the conditions described in table 1. The indirect mechanism plays a minor role, if any, in the low temperature conversions described in this report.

This study suggests that coke formation via equations (5) and (6) and metal oxide aggregation are the main problems to be overcome for producing a low temperature direct oxidation catalyst with a long lifetime.

Acknowledgement

The authors acknowledge the support of this research by the Amoco–Intevep Cooperative Natural Gas Program.

References

[1] (a) J.R. Rostrup-Nielsen, Catal. Today 18 (1993) 305;
(b) D.A. Hickman and L.D. Schmidt, J. Catal. 138 (1992) 267;
(c) S.S. Bharadwaj and L.D. Schmidt, J. Catal. 146 (1994) 11;
(d) O.V. Krylov, Catal. Today 18(3) (1993) 209;
(e) J.M. Fox III, Catal. Rev. Sci. Eng. 35(2) (1993) 169.

[2] M.V. Twigg, ed., *Catalyst Handbook* (Wolfe, London, 1989).

[3] R.F. Blanks, T.S. Wittrig and D.A. Peterson, Chem. Eng. Sci. 45 (1990) 2407.

[4] A.T. Ashcroft, A.K. Cheetham, J.S. Foord, M.L.H. Green, C.P. Grey, A.J. Murrell and P.D.F. Vernon, Nature 344 (1990) 319.

[5] P.D.F. Vernon, M.L.H. Green, A.K. Cheetham and A.T. Ashcroft, Catal. Lett. 6 (1990) 181.

[6] A.T. Ashcroft, A.K. Cheetham, M.L.H. Green and P.D.F. Vernon, Nature 352 (1991) 225.

[7] R.H. Jones, A.T. Ashcroft, D. Waller, A.K. Cheetham and J.M. Thomas, Catal. Lett. 8 (1991) 169.

[8] D. Dissanayake, M.P. Rosynek, K.C.C. Kharas and J.H. Lunsford, J. Catal. 132 (1991) 117.

[9] A. Balakrishna, L.D. Schmidt and R. Aris, Chem. Eng. Sci. 49 (1994) 11.

[10] A.K. Bhattacharyya, J.A. Breach, S. Chand, D.K. Ghorai, A. Hartridge, J. Keary and K.K. Mallick, Appl. Catal. 80 (1992) L1.

[11] V.R. Choudhary, A.M. Rajput and B. Prabhakar, J. Catal. 139 (1993) 326.

[12] D. Dissanayake, M.P. Rosynek and J.H. Lunsford, J. Phys. Chem. 97 (1993) 3644.

[13] D.A. Hickman and L.D. Schmidt, Science 259 (1993) 343.

[14] (a) D.A. Hickman, E.A. Haupfear and L.D. Schmidt, Catal. Lett. 17 (1993) 223;
(b) P.M. Tarniainen, X. Chu and L.D. Schmidt, J. Catal. 146 (1994) 1.

[15] M. Prettre, C. Eichner and M. Perrin, Trans. Faraday Soc. 43 (1946) 355.

[16] A. Bhattacharyya and V.W. Chang, in: *Studies in Surface Science and Catalysis*, eds. B. Delmon and G.F. Froment (Elsevier, Amsterdam, 1994) pp. 207–213.

[17] M.A. Pena, J.P. Gomez and J.L.B. Fierro, Appl. Catal. A 144 (1996) 7.

[18] (a) I. Alstrup and M.T. Tavares, J. Catal. 135 (1992) 147;
(b) J.B. Claridge, M.L.H. Green, S.C. Tsang, A.P.E. York, A.T. Ashcroft and P.D. Battle, Catal. Lett. 22 (1993) 299.

[19] (a) M. Houalla, F. Delannay, I. Matsuura and B. Delmon, J. Chem. Soc. Faraday I 76 (1980) 2128;
(b) J.C. Verdine, G. Hollinger and T.M. Duc, J. Phys. Chem. 82 (1978) 1515.

[20] M. Montes, J.B. Soupart, M. De Saedeleer, B.K. Hodnett and B. Delmon, J. Chem. Soc. Faraday I 80 (1984) 3209.

[21] J.P. Espinos, A.R. Gonzalez-Elipe, A. Caballero, J. Garcia and G. Munuera, J. Catal. 136 (1992) 415.

[22] (a) M. Houalla, F. Delannay and B. Delmon, J. Chem. Soc. Faraday I 76 (1980) 1766;
(b) M. Wu and D.M. Hercules, J. Phys. Chem. 83 (1979) 2003.

[23] R.A. Svehla and B.J. McBride, Fortran IV computer program for calculation of thermodynamic and transport properties of complex chemical systems; COSMIC Program #Lew-11997, NASA TN D-7056 (January 1973).

[24] F. van Looij and J.W. Geus, J. Catal. 168 (1997) 154.